OFFICE OF NAVAL RESEARCH

Grant N00014-89-J-1178

R&T Code 413Q001-05

TECHNICAL REPORT No. #46

A New Ellipsometry Technique For Interface Analysis: Application To $Si-SiO_2$

By:

E. A. Irene and V. A. Yakovlev*
Department of Chemistry
University of North Carolina at Chapel Hill
Chapel Hill, NC 27599-3290

*Institute of Crystallography, Acad. of Sci., Leninsky pr. 59
Moscow, 117333 RUSSIA

Presented at Second Symposium on Chemistry and Physics of SiO_2 and $Si-SiO_2$ Interface and to be Published 1993 in Symposium Volume.

July 13, 1992

REPORT DOCUMENTATION PAGE

Form Approved
OMB No. 0704-0188

1. AGENCY USE ONLY *(Leave blank)*	2. REPORT DATE	3. REPORT TYPE AND DATES COVERED
	July 13, 1992	

4. TITLE AND SUBTITLE
A New Ellipsometry Technique for Interface Analysis: Application to Si-SiO_2

5. FUNDING NUMBERS
#N00014-89-J-1178

6. AUTHOR(S)
E.A. Irene and V. A. Yakovlev

7. PERFORMING ORGANIZATION NAME(S) AND ADDRESS(ES)
The University of North Carolina
Chemistry Department
CB# 3290, Venable Hall
Chapel Hill, NC 27599-3290

8. PERFORMING ORGANIZATION REPORT NUMBER

9. SPONSORING/MONITORING AGENCY NAME(S) AND ADDRESS(ES)
Office of Naval Research
800 N Quincy Street
Arlington, VA 22217-5000

10. SPONSORING/MONITORING AGENCY REPORT NUMBER
Technical Report #46

11. SUPPLEMENTARY NOTES
none

12a. DISTRIBUTION/AVAILABILITY STATEMENT
This document has been approved for public release and sale, distribution of this document is unlimited.

12b. DISTRIBUTION CODE

13. ABSTRACT *(Maximum 200 words)*

In this paper we report a new spectroscopic ellipsometry technique that overcomes much of the ambiguity associated with measuring an interface under a film. For this technique we match the refractive index of the overlayer with an immersion liquid and then perform spectroscopic ellipsometry at several angles of incidence. Essentially, the overlayer is optically (not physically) removed, thereby rendering the ellipsometric measurement sensitive to the interfacial layer which is often known to be optically and chemically different than either substrate or film. The Si-SiO_2 interface resulting from thermal oxidation of Si, and the evolution of the interface with annealing is studied using the new technique.

14. SUBJECT TERMS	15. NUMBER OF PAGES
plasmas, oxidation	
	16. PRICE CODE

17. SECURITY CLASSIFICATION OF REPORT	18. SECURITY CLASSIFICATION OF THIS PAGE	19. SECURITY CLASSIFICATION OF ABSTRACT	20. LIMITATION OF ABSTRACT
unclassified	unclassified	unclassified	

A NEW ELLIPSOMETRY TECHNIQUE FOR INTERFACE ANALYSIS: APPLICATION TO $Si-SiO_2$

E.A. Irene and V.A. Yakovlev*

Department of Chemistry CB# 3290
University of North Carolina
Chapel Hill, NC 27599-3290

* Institute of Crystallography, Acad. of Sci., Leninsky pr. 59 Moscow 117333 Russia

ABSTRACT

In this paper we report a new spectroscopic ellipsometry technique that overcomes much of the ambiguity associated with measuring an interface under a film. For this technique we match the refractive index of the overlayer with an immersion liquid and then perform spectroscopic ellipsometry at several angles of incidence. Essentially, the overlayer is optically (not physically) removed, thereby rendering the ellipsometric measurement sensitive to the interfacial layer which is often known to be optically and chemically different than either substrate or film. The $Si-SiO_2$ interface resulting from thermal oxidation of Si, and the evolution of the interface with annealing is studied using the new technique.

INTRODUCTION

It is apparent that the interface region between a semiconductor surface and a film, particularly dielectric films for MOSFET devices, is of crucial importance. Consequentially, the interface region of electronically relevant films on semiconductors has been widely studied by a variety of techniques (see for example ref 1 and refs 1-29 in ref 1). These techniques fall into a few broad classes that will be briefly discussed with the use of Fig.1. First, there are the optical techniques that can access the optical response of the interface through an optically transparent overlayer, as seen in Figure 1a. While many successful studies have been done with the optimization of this technique, particularly ellipsometry studies, the key drawback is that the optical signals from the top interface must somehow be taken care of (minimized or subtracted etc.), in order to extract purely interface information. Second, there are techniques that can observe a surface with the overlayer somehow removed. Typically, the overlayer can be chemically etched or

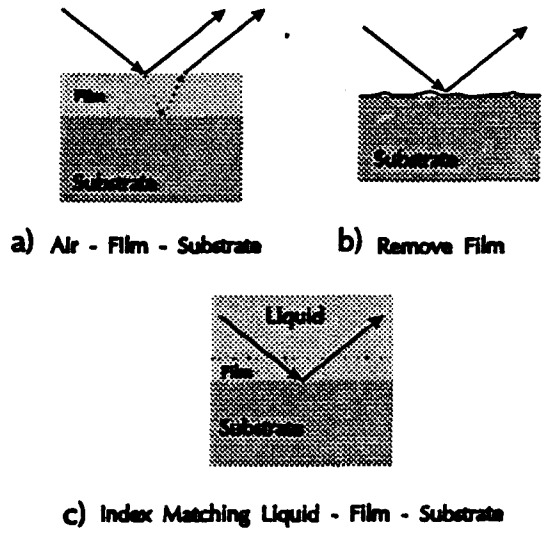

Figure 1. Comparison of interface analysis methods.

physically sputtered or a combination. Figure 1b indicates that the interface region can be altered by these aggressive processes, and that the information obtained about a previous interface contains an ambiguity. There are intermediate techniques such as cross-sectional transmission electron microscopy, XTEM, which neither removes the overlayer nor is overly sensitive to extraneous sources of signal. However, this technique requires considerable sample preparation, in particular the sample thinning, which can alter the interface. Notwithstanding the limitations of each technique, and taken in total, these techniques have contributed significantly to our understanding of the important interfaces.

The present paper deals with the development and application of a novel in-situ ellipsometry technique that can access the interface region for an optically transparent film on a surface[1,2]. The principle of operation of the technique is to immerse the film covered substrate sample in a liquid that refractive index matches to the overlayer film as illustrated in Figure 1c. In this way, the optical response consists only of reflections from the film-substrate interface region thereby removing the above mentioned ambiguity. It is assumed that the interface region is optically distinct from either the bulk film and substrate, an assumption borne out in many studies. The enhanced sensitivity of the technique will be demonstrated. By way of application, the Si-SiO_2 interface is chosen and the nature and evolution of this interface is examined as a function of thermal annealing.

THE TECHNIQUE

Index Matching. The ideal immersion liquid should be non reactive and transparent over a wide spectral range. Both the refractive index and the dispersion must correspond to the average refractive index of the overlayer. The refractive indices for the immersion liquids were calculated using a three term Cauchy dispersion formula, taking into account temperature and using literature values for the various constants[3,4]. Using liquid mixtures it is possible to adjust the refractive indexes of the ambient to that for SiO_2. Figure 2 shows the spectral dependencies of the refractive index of pure carbon tetrachloride, CCl_4, benzene, C_6H_6, and mixtures[3]. Both CCl_4 and C_6H_6 are nonpolar organic liquids that do not interact with SiO_2. Also in Figure 2 is shown the calculated spectral dependencies of the refractive index of bulk and thin film SiO_2 calculated using a single term Sellmeier approximation after Jellison[5]. Since n for thermally grown SiO_2 films is dependent on the thickness[6,7], the use of immersion liquids with different refractive indexes corresponding

to the average refractive indexes of the films under investigation renders accuracy improvements possible.

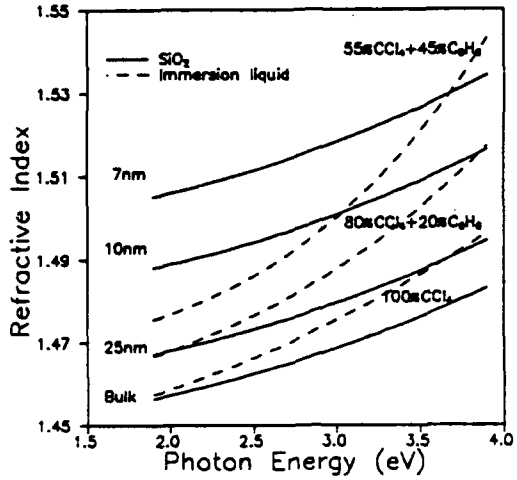

Figure 2. The refractive index versus photon energy for pure carbon tetrachloride (CCl_4), and mixtures with benzene (C_6H_6), along with bulk and thin-film SiO_2.

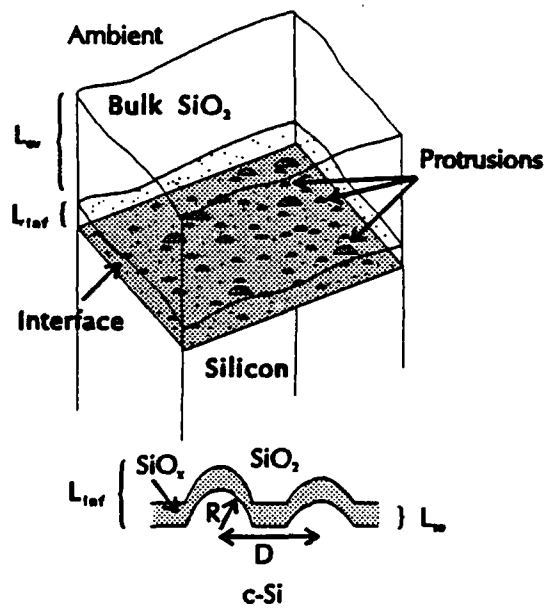

Figure 3. Model for the substrate-interface-overlayer-ambient system.

Analysis. In order to assess the sensitivity of the technique, the complicated structure shown in Figure 3 and thought to represent the Si-thermally grown SiO_2 system is simplified to a two film system with interface and overlayer thicknesses L_{inf} and L_{ov}, respectively. Thus, at this juncture the interface region in Figure 3 is considered to be a homogenous layer with an effective dielectric function, ϵ_{inf}. The overlayer or bulk SiO_2 film is represented with an average refractive index n_{ov}. The complex reflection coefficient, ρ, for the system is given by:

$$\rho = \tan\Psi \exp(i\Delta) = \rho(\lambda, \phi, n_o, n_{ov}, n_s, k_s, \epsilon_{inf}, L_{ov}, L_{inf}) \quad (1)$$

where Ψ, Δ are the ellipsometric measurables and the terms in the parenthesis on the right are parameters, some known a priori and some to be determined. The maximum change in ρ, $\delta\rho/\rho$, is the condition of optimum sensitivity in the measurables, Δ, Ψ. It is desirable to determine the optimum sensitivity in terms of the controllable parameters: angle of incidence, ϕ, and wavelength of light, λ. From the analytical solution for optimized ellipsometric measurements of interfaces with thicknesses, $L_{inf} << \lambda/4$ in a thin film

structure[8], it was shown that the condition of $\delta\rho/\rho$ divergence or maximum sensitivity is:

$$r_{01}^{p(and s)} + r_{12}^{p(and s)} \exp(-2i\beta) = 0 \quad (2)$$

where the r's are the Fresnel reflection coefficients with subscripts corresponding to the interface between the media with numbering starting from 0 with the ambient and β is given as:

$$\beta = \frac{2\pi L_{ov}}{\lambda}\sqrt{(n_{ov}^2 - n_o^2 \sin^2\phi)} \quad (3)$$

It should be observed that the properties of the interface do not influence the best sensitivity conditions.

If the refractive index of the ambient is close to the index of the overlayer, i.e. $n_o \approx n_{ov}$, then $r_{01} \approx 0$. The optimum sensitivity condition from eqn(2) becomes r_{12} or, taking into account $n_o \approx n_{ov}$, $r_{02} \approx 0$. For the p wave this condition is equal to a minimum of the ellipsometric angle, $\Psi(\phi,\lambda)$[9].

We determine the optimal spectral range and angles of incidence from a simulation of $\Psi(\phi,\lambda)$ and $\Delta(\phi,\lambda)$ dependencies using the model in Figure 3 for the Si-SiO_2 system with the following assumptions: a. crystalline Si substrate with known dielectric function[9]; b. interface microroughness (see Figure 3) with effective height of 0.2nm and composition of 50% c-Si and 50% suboxide SiO_x, with x = 0.4 and the Bruggeman effective medium approximation, BEMA, was used to calculate a dielectric function of the mixture; c. interface suboxide transition zone of 0.6nm composed of $SiO_{0.4}$; d. SiO_2 overlayer with an average refractive index $n_{ov}(L_{ov})$; e. an air or pure CCl_4 ambient with refractive index n_o.

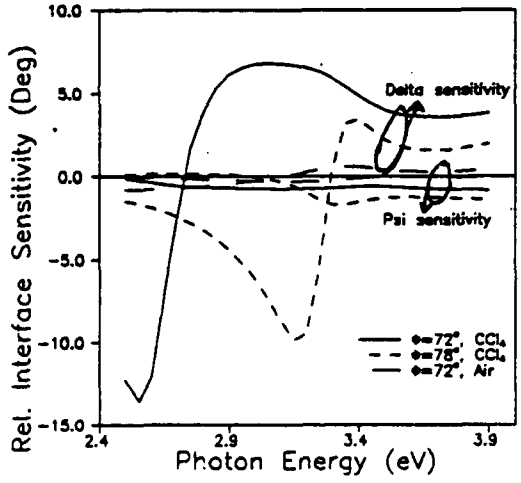

Figure 4. Relative interface sensitivity for Δ and Ψ for air and CCl_4 ambients.

Figure 4 shows a plot of the interface sensitivity for both Ψ and Δ in terms of a relative interface sensitivity function $\delta\Delta(E) = \Delta_0(E) - \Delta_{inf}(E)$ for air and CCl_4 ambients. Where $\Delta_0(E)$ and $\Delta_{inf}(E)$ were calculated for the cases without and with an interface layer, respectively. It is seen that the sensitivity of Δ to the presence of an interfacial layer is increased by more than an order of magnitude with the parameters at optimum sensitivity, but the Ψ sensitivity is low. However, changing ϕ to 78° for the same system enhances the Ψ sensitivity to the interfacial layer and this is also shown in Figure 4.

Calculation Scheme. In order to find unknown parameters of the modeled interface, we used the Marquardt non-linear best-fit algorithm which minimizes the value of the error function:

$$Q = \sum_{ij} [(\Delta_{ij}^{cal}(\phi_i, E_j, P) - \Delta_{ij}^{exp})^2 + (\Psi_{ij}^{cal}(\phi_i, E_j, P) - \Psi_{ij}^{exp})^2] \quad (4)$$

where P is a vector of N unknown interface parameters and E_j is the photon energy, and the superscripts cal and exp refer to calculated and experimentally derived values. Δ^{cal} and Ψ^{cal} are the values obtained using the vector P, the Fresnel formulas[10] and a matrix algorithm for the multilayer system complex reflection coefficient. Optical parameters for the immersion liquid and SiO_2 overlayer included in the fitting procedure were calculated from dispersion equations mentioned above. BEMA was used to calculate the effective dielectric function for a mixture of constituents with known optical properties. Volume fractions of the constituents are treated as unknown parameters.

The calculation returns the vector P when an initial guess, P^o, is input, i.e. the program returns a value of P at the local minimum of Q, near the initial value. In addition, correlations between the fitting parameters are expressed in terms of the correlation matrix of the derivatives $\partial\Psi/\partial p_n$, $\partial\Delta/\partial p_n$ and a 95% confidence limit was used to calculate errors in the fitting parameters.

EXPERIMENTAL PROCEDURES

A commercially available vertical ellipsometer bench was modified to become rotating analyzer spectroscopic ellipsometer with the details previously described[11] and calibrated according to a published procedure[12] and the details described[1]. Calibration was performed on a sample with $\Delta \approx 90°$ (Si wafer with thermally grown SiO_2 film) both in air and in the immersion cell in liquid.

A fused silica immersion cell, as shown in Figure 5, has been designed for the variable angle of incidence and spectroscopic measurements. The most significant feature of the cell is that the two optically flat and annealed fused silica plates, serving as the entrance and exit windows, are connected rigidly to the polarizer and analyzer arms, but not to the cell. The windows were adjusted to be exactly orthogonal to the incident light at the straight-through position of the ellipsometer (ϕ=90°), in order to avoid any deviation of the incident light beam when it passes through adjacent media with different indexes. Two fitted metal tubes in each arm permit some lateral movement of the window position without a change of the window tilt. The cell is rigidly attached to a stage and connected to the tubes using chemically inert flexible tubing. A change of ϕ in the range of 67°-90° is possible while maintaining the window alignment precision during the immersion measurements.

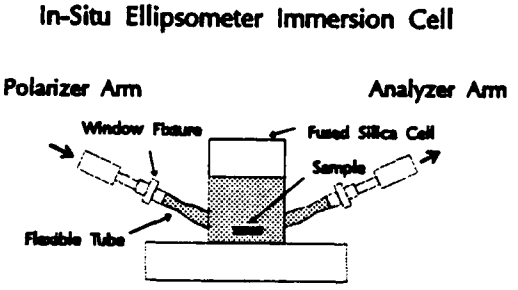

Figure 5. Sketch of the variable angle of incidence immersion cell.

Single-crystal (100) oriented 2 Ωcm p-type silicon wafers were cleaned prior to oxidation using a slightly modified RCA cleaning procedure[13]. The samples were thermally oxidized to about 20nm at 800° C in a fused silica tube furnace in clean dry oxygen which yielded MOS quality SiO_2 films on Si. For the annealing studies, after a particular oxidation, one sample was removed without annealing as a control, and the others were annealed in a clean nitrogen atmosphere for annealing temperatures and times in the range 750-1100°C and 1-120 min, respectively.

In order to use the convergence routines, an estimation of the overlayer thickness

is required. One layer (substrate-overlayer) and two layer (substrate-interface-overlayer) models have been used to analyze the spectroscopic ellipsometry scans of the about 25nm SiO_2 films on Si samples in air. From these measurements in air, the difference in the minimum error function, Q, for one and two layer models was negligible, which indicates low interface sensitivity. However, these measurements yield a good estimate of the overlayer thickness to a precision of better than 0.5%. The refractive index of the film was calculated from dispersion relations. Immersion measurements were performed in pure CCl_4 at 20°C. Carbon tetrachloride becomes nontransparent at energies higher than ~4 eV which then defines the upper limit of the spectral range to be 4eV. The precision of rotating analyzer ellipsometry without using an achromatic compensator falls significantly when Δ approaches 180° or 0° [14]. To avoid this situation, we have used 2.5 eV as the lower energy limit where Δ is more than 20°. Therefore, Δ is restricted to $20° < \Delta < 160°$ in the spectral range 2.5-4.0 eV for the measurements in the immersion liquid at the angles of incidence ϕ = 70°-80°.

RESULTS: Evolution of the Si-SiO_2 Interface During Annealing.

Model Independent Results. A series of annealing experiments were performed on SiO_2 covered Si samples, and the results are first displayed without recourse to a model, so that an objective view of the interface evolution can be obtained. Figures 6 and 7 display experimental results in terms of the interface parameter $\delta\Delta_{inf}(T_{an}, t_{an})$ defined as:

$$\delta\Delta_{inf}(T_{an}, t_{an}) = \Delta^{exp}(T_{an}, t_{an}) - \Delta_o^{exp} - \delta\Delta_{ov}^{cal}(T_{an}, t_{an}) \qquad (5)$$

where $\Delta^{exp}(T_{an}, t_{an})$ is the experimental ellipsometric angle Δ at a specific annealing temperature and time, Δ_o is the ellipsometric angle for a non-annealed sample and the term $\delta\Delta_{ov}^{cal}(T_{an}, t_{an})$ is the overlayer relaxation correction. This correction term represents the difference in Δ for the single-film (without interface) system of a non-annealed and

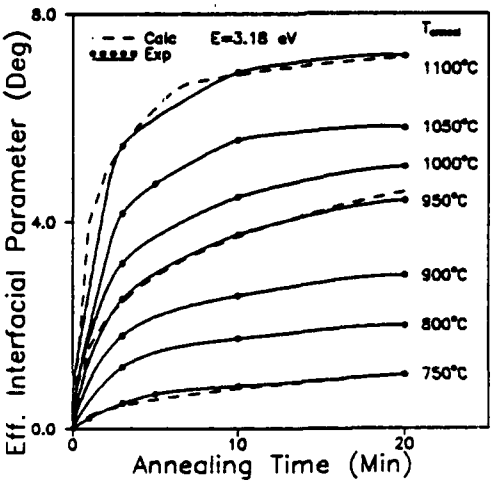

Figure 6. The experimental dependence of the effective interface parameter, Δ_{inf}, on annealing time at a number of annealing temperatures. A simulated dependency is shown with the dashed curve.

annealed overlayer with the refractive index calculated from a consideration of stress relaxation[6,15,16,17], and represents only a few percent of $\delta\Delta_{inf}$. The chosen photon energy E=3.18 eV is in the range of the maximum interface and the minimum overlayer sensitivity. Figure 6 shows the values for $\delta\Delta_{inf}$ measured at 3.18 eV versus anneal time at a number of temperatures, and versus anneal temperature at two times in Figure 7. Other information relating to modelling is also included in Figure 6, but discussion of these items will be deferred. It is seen in Figure 6 that at all annealing temperatures two

temporal regions of behavior are present. Initially, the anneals yield a relatively fast

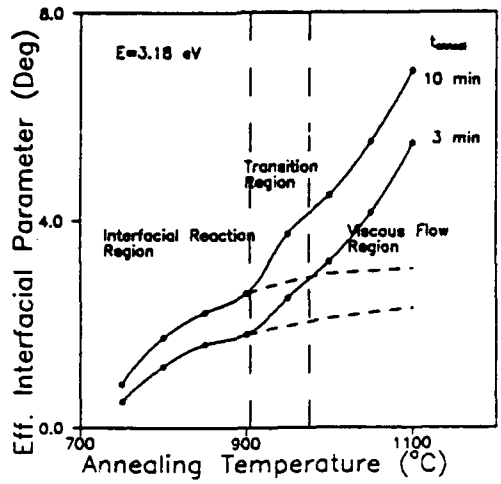

Figure 7. The experimental dependence of the effective interface parameter, Δ_{inf}, on annealing temperature for two annealing times.

increase in $\delta\Delta_{inf}$ that slows after 5 min and then nearly saturates. The data in Figure 7 is from Figure 6 at two anneal times, one before and one near saturation, and this plot versus anneal temperature reveals a distinct break in the 900°-970°C range, which corresponds to the viscous flow range, i.e. a temperature above which viscous flow of the oxide is fast[18]. Thus, we consider that the viscous relaxation dominates at the higher anneal temperatures, but at lower temperatures where a large part of the change in $\delta\Delta_{inf}$ occurs, we need to consider other possible mechanisms.

If the interface region is treated as a single homogenous film, then the extent of the interface is observed to decrease with both annealing time and temperature as evidenced by the increasing Δ_{inf}. With both a decrease in the interface region for short and long times and low and high temperatures, the model that is chosen for the different modes of behavior must show the observed functionality.

An Interface Model. Previous models for the Si-SiO_2 interface have agreed that the interfacial region is structurally and chemically different from either Si or SiO_2. Components of the interfacial region include roughness and a suboxide, SiO_x, as is shown in Figure 3. The parameters that quantify this working model, and then the experimental data $\Delta^{exp}(E,\phi,T_{an},t_{an})$, $\Psi^{exp}(E,\phi,T_{an},t_{an})$ are reduced to yield values for the model parameters which are compared with other studies about the interface region. We describe the roughness by crystalline silicon protrusions as hemispheres with an average radius R, which form a hexagonal network with an average distance D between centers. The protrusions and the region between them are covered by a layer of suboxide, SiO_x, with $0<x<2$, and with an average thickness L_{so}. The effective thickness of the complex transition layer is given as:

$$L_{inf} = R + L_{so} \qquad (6)$$

and an effective dielectric function ϵ_{inf}, which represents a mixture of crystalline silicon c-Si, silicon suboxide SiO_x and the SiO_2 overlayer and written as:

$$\epsilon_{inf} = \epsilon_{inf}(\epsilon_{c\text{-}Si}, f_{c\text{-}Si}, \epsilon_{SiO_x}, f_{SiO_x}, \epsilon_{SiO_2}, f_{SiO_2}) \qquad (7)$$

ϵ_{inf} was calculated using the BEMA, where the dielectric properties, ϵ, and relative volume fractions, f, of all of the interfacial layer constituents are known a priori. The dielectric function of SiO_x was calculated[1,2] using the BEMA, and by considering that SiO_x is a mixture of a-Si, and SiO_2[19].

In order to model the evolution of the interface during annealing, we use a power law to describe the reduction of both the protrusions and the chemical transition layer with the powers p and g respectively are taken to be p=g=0.5 which implies a diffusion model and is justified below.

The minimization of the error function (eqn.(4)) for the sets of experimental data for the non-annealed wafer at ϕ=72° and 75° gives the average distance between the centers of protrusions D = 44±4 Å, initial radius of the protrusions R° = 9.8±0.3 Å and initial thickness of suboxide, SiO, L_{so} = 3.4±0.2 Å. These results are in agreement with the interface geometry sensitive TEM study of the SiO_2-Si, which shows that distances between protrusions at non-annealed interface are distributed in the range 40-50 Å and heights are 9-15 Å[20]. Also, photoelectron spectroscopy revealed a chemical transition layer with a thickness of 2.4-4 Å[21].

A simulation of the kinetic dependencies, $\delta\Delta_{inf}(T_{an}, t_{an})$, with p=g=0.5 yields close agreement (dashed lines in Figure 6) with the experimental plots of $\delta\Delta_{inf}(t_{an})$.

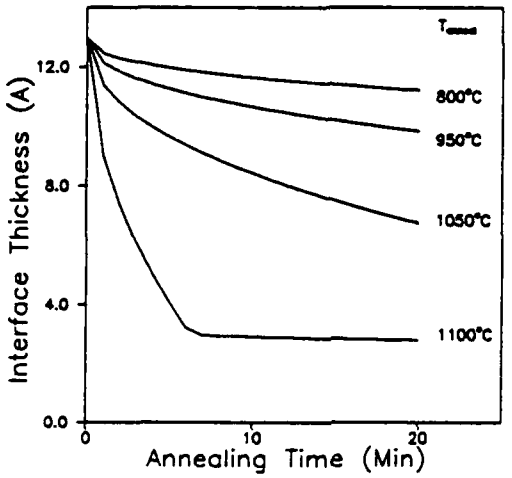

Figure 8. The dependence of the effective interface thickness on annealing time at a number of annealing temperatures.

Figure 8 displays the decrease of the extent of the interface, L_{inf}, i.e. effective thickness from eqn.(6) with a minimum thickness of about 3 Å realized at the highest anneal temperatures. The interface effective refractive index vs t_{an} at several T_{an} is shown in Figure 9.

Initially both the index and thickness of the interface layer decrease due to the shrinking of the silicon protrusions. This is followed by the slower decrease of the SiO_x transition layer which becomes dominant after considerable reduction of the height of the protrusions. The sharp increase in the index seen in Figure 9 for the 1100°C annealed sample is indicative of the index returning quickly to the SiO value as the fraction of the Si as protrusions in the interface layer rapidly goes to zero. The same effect would occur for the other anneal temperatures but more slowly. A slower rise in index is seen for the 1050°C annealed sample after 10 min and the time is too short to see the rise for the lower temperature anneals. The overall shape of the results in Figure 9 is typical of and dictated by the BEMA model used to interpret the data.

The results show two distinct modes for the evolution of the Si-SiO_2 interface upon annealing. The low temperature mode corresponds to a reduction in the suboxide and protrusions. The coefficients, p and g that scale this evolution yield an excellent fit to the data when a value of 0.5 is used in modelling. This suggests that Si atom diffusion is operative for the smoothening reaction and inward trace oxidant diffusion for the suboxide disappearance. At high temperatures these reactions occur but the dominant mode is viscous relaxation of the oxide overlayer. These model dependent assertions are consistent

with other studies and are shown to be accessible by the novel ellipsometric technique herein described.

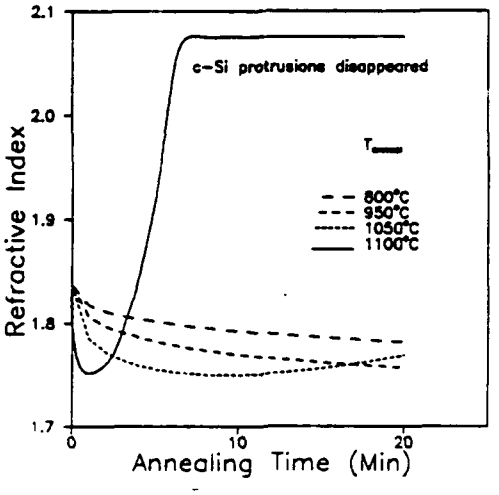

Figure 9. The dependency of the effective interface refractive index on annealing time at a number of annealing temperatures.

ACKNOWLEDGEMENTS

This research was supported in part by the Office of Naval Research, ONR.

REFERENCES

1. V.A. Yakovlev and E.A. Irene, J. Electrochem. Soc.,139, 1450 (1992).

2. V.A. Yakovlev, Q. Liu and E.A. Irene, J. Vac. Sci. and Tech. A, 10(3), May/June (1992).

3. "Techniques of Chemistry", Ed. A. Weissberger, Vol.II Organic Solvents, Ed. J.A. Riddick and W.B. Bunger, Wiley-Interscience, NY, 1970.

4. P.Perez, T.E.Block, and C.M.Knobler, J. Chem. and Engineering Data, 16, 333 (1971).

5. G.E.Jellison, Jr., J. Appl. Phys., 69, 7627 (1991).

6. A.Kalnitsky, S.P.Tay, J.P.Ellul, S.Chongsawangvirod, J.W.Andrews, and E.A.Irene, J. Electrochem. Soc., 137, 234 (1990).

7. S.Chongsawangvirod, E.A.Irene, A.Kalnitsky, S.P.Tay, and J.P.Ellul, J. Electrochem. Soc., 137, 3536 (1990).

8. S.A.Alterovitz, G.H.Bu-Abbud, and J.A.Woollam, Thin Solid Films, 128, 183 (1985).

9. D.E.Aspnes, A.A.Studna, Phys. Rev. B: Condensed Matter, 27, 985 (1983).

10. R.M.A.Azzam and N.M.Bashara, "Ellipsometry and Polarized Light", North-Holland, Amsterdam, 1977.

11. X.Liu, J.W.Andrews, and E.A.Irene, J. Electrochem. Soc., 138, 1106 (1991).

12. J.M.M. de Nijs, A.H.M.Holtslag, A.Hoeksta, and A. van Silfhout, J. Opt. Soc. Am. A, 5, 1466 (1988).

13. W.Kern and D.A.Puotinen, RCA Rev., 31, 187 (1970).

14. D.E.Aspnes, J. Opt. Soc. Am., 64, 639 (1974).

15. E.A.Irene, E.Tierney, and J.Angillelo, J. Electrochem. Soc., 129, 2594 (1982).

16. L.M.Landsberger and W.A.Tiller, Appl. Phys. Lett., 51, 1416 (1987).

17. K.Taniguchi, M.Tanaka, C. Hamaguchi, and K.Imai, J. Appl. Phys., 67, 2195 (1990).

18. E.P.EerNisse, Appl. Phys. Lett, 35, 8 (1979).

19. G.Zuther, Phys. St. Sol.(a), 59, K109 (1980).

20. H.Akatsu, Y. Sumi, and I. Ohdomari, Phys. Rev. B, 44, 1616(1991).

21. T.Hattori and T.Suzuki, Appl. Phys. Lett., 43, 470 (1983).